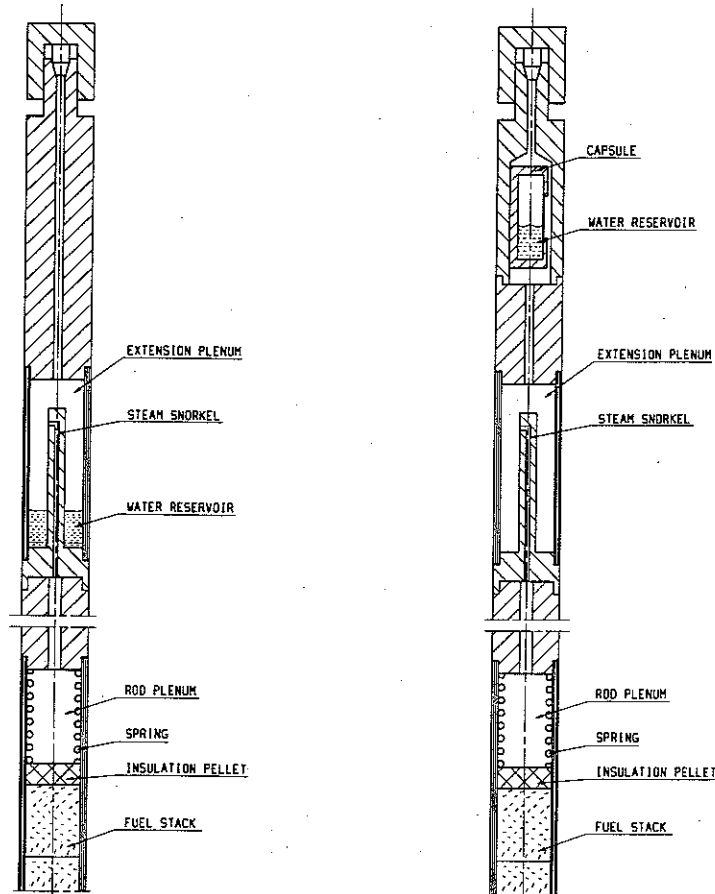


STUDIES OF SECONDARY HYDRIDING IN BWR TEST FUEL

European Working Group
"Hot Laboratories and Remote Handling"

Plenary Meeting, June 5-6, 1997, Studsvik Nuclear AB
Hot Cell Laboratory, SE-611 82 Nyköping, Sweden

Christian Gräslund, Anders Lassing



Studies of secondary hydriding in BWR test fuel

by Christian Gräslund and Anders Lassing, Studsvik Nuclear AB

Presented at the European Working Group "Hot Laboratories and Remote Handling" Plenary Meeting June 5 and 6, 1997, at Studsvik, Sweden

ABSTRACT

A total of 20 tests have been performed in the R2 reactor with the aim to study secondary hydriding of cladding caused by water from a simulated primary defect in test rodlets of 8x8 BWR design. Three kinds of Zircaloy-2 cladding have been compared, namely standard cladding, cladding with unalloyed zirconium liner and so called *rifled* cladding, which is a proposed remedy.

18 tests were carried out with previously unirradiated test fuel in two exploratory test series, DEF-1 and DEF-2, and in the DEFEX Project. In these tests the intrusion of water through the primary defect was simulated by applying an open water reservoir in an extended plenum on top of the rodlet in the DEF and DEFEX tests.

In order better to simulate defection of a rod during operation, the technique was modified in the last two DEMO tests with irradiated fuel of medium burnup. The water was contained in a closed ampoule in the extended plenum, and the ampoule was made to burst when the test rodlet had been irradiated at full power for a predetermined period of time. The rodlets were refabricated at the Hot Cell Laboratory using the STUDFAB process.

Neutron radiography, eddy current scanning and profilometry measurement at the R2 reactor showed that most of the hydrides and the cracks developed in the lower part of the rodlets. Subsequent PIE was done at the Hot Cell Laboratory. Visual inspection showed that only in the DEMO tests did the cracks grow outside the hydrided region. Gamma scanning of the rodlets was performed after each test in order to determine the distribution of fission products and the average power profile during irradiation. Investigation by SEM gave hydride distribution and oxide thickness. Ceramography was done optically for porosity and grain size measurement. Metallography was also performed. X-ray powder diffraction was used to determine the hyperstoichiometry of the uranium dioxide. For those rodlets that did not fail, the internal gas was analysed with respect to remaining hydrogen and fission gases.

List of Contents

	Page
1	Introduction 1
2	Overview of defect fuel experiments at Studsvik 1
2.1	Experimental programs 1
2.2	Objectives 1
2.3	Mechanism for formation of secondary defects 2
3	Experimental technique 3
3.1	Accomplishing steam starvation conditions 3
3.2	Simulation of primary defect 3
3.3	The new type of water capsule 3
4	Test procedure 5
4.1	Design parameters 5
4.2	Experimental parameters 5
5	Results 6
5.1	Outcome of tests 6
5.2	Post-irradiation gamma scanning 7
5.3	Post-irradiation SEM analysis 7
5.4	Post-irradiation ceramography 9
5.5	Post-irradiation stoichiometry measurement 9
5.6	Post-irradiation analysis of internal gas 10
6	Conclusions 11
	References 12
	Tables 13
	Figures 16

1 Introduction

Several fuel failures in BWR and PWR nuclear power plants have been reported and analyzed. In recent years the predominant causes in BWRs for primary defects have been fretting by loose debris in the system and PCI. Similarly, debris fretting and grid - rod fretting account for most of the primary failures in PWRs. Other causes, such as manufacturing flaws have also been identified [1]. In a number of cases, primary defects in the fuel have led to the development of secondary defects because of internal hydriding. If these lead to long longitudinal splits or circumferential breaks, extensive releases of fission products and even of fuel material may occur.

2 Overview of defect fuel experiments at Studsvik

2.1 Experimental programs

From 1990 to 1993 seven tests with previously unirradiated fuel were run in two series, DEF-1 and DEF-2 [2, 3]. With the results from these tests the DEFEX Project was conducted in international co-operation between 1993 and 1995. A total of 11 tests on unirradiated fuel were carried out within this program [4]. In the autumn of 1996 two more **DEMO** tests on fuel with medium burnup were made with a modified test method [5].

2.2 Objectives

The objectives of the exploratory two DEF Projects were demonstration of the experimental technique applied to different types of cladding. In the DEFEX Project the aim was further elaborated to be investigation of phenomena and design parameters relevant to the degradation process in defected fuel. In particular, the collected data should be used for modeling of defect fuel behavior, thus providing a theoretical and experimental basis for further testing of potential remedies.

In the DEF and DEFEX tests Zircaloy-2 standard and liner cladding were compared to *rifled* cladding, the latter being characterized by the polygonal shape of the bore cross-section, which is intended to prevent secondary hydriding by facilitating axial gas communication.

The concluding two tests aimed at accomplishing cracks propagating from hydrided regions in standard Zircaloy-2 cladding. Destructive investigation of the cracks would give information on the mechanism for crack propagation in irradiated cladding.

2.3 Mechanism for formation of secondary defects

The mechanism for secondary hydriding has been evaluated [i.a. 6, 7], and the following hydriding criterion for the partial pressures of steam and hydrogen reacting with Zircaloy in a stagnant system under steam starvation conditions at reactor temperatures has been arrived at:

$$\frac{P_{\text{H}_2\text{O}}}{P_{\text{H}_2}} < 0.01 \text{ assuming that } P_{\text{H}_2} \geq 20 \text{ mm Hg.}$$

The failure degradation scenario that has been proposed starts with water penetrating the cladding through the primary defect, flashing into steam and filling the fuel - cladding gap and the plenum. In general, the internal steam pressure will reach the system pressure rather rapidly. The steam oxidizes the fuel and the internal surface of the cladding, thus producing an increasing amount of hydrogen, some of which will be picked up by the cladding. In the beginning the production of hydrogen is dominated by fuel oxidation. The process is also influenced by radiolysis of water producing peroxide and hydrogen and by the presence of fission products.

The fuel - cladding gap is partly closed, and the closure depends on the linear heat rate, LHR, and the burnup. The resulting constriction will cause most of the steam to be reduced at some axial distance from the defect, thus fulfilling the steam starvation criterion at this location. After an incubation period the protective oxide layer on the inner surface of the cladding is penetrated, and hydrogen can enter the cladding, before the layer is repaired. This accelerated hydriding can continue as massive localized hydriding. Because of its lower density the resulting aggregate of δ -phase hydride produces internal stresses which may lead to secondary failure of the cladding. The fact that the hydride is brittle enhances the possibility of through-going cracks.

3 Experimental technique

3.1 Accomplishing steam starvation conditions

Since the active height of the R2 reactor is 600 mm, the length of the test rodlets has to be less than that. Because of the axially peaked power profile, there will be a section at the middle of the rodlets where there is strong mechanical interaction between the cladding and the fuel. As result the water vapor entering from above will be prevented from reaching the lower part. Some downward diffusion will occur, but due to oxidation of the UO_2 and the cladding, the steam will be reduced to hydrogen. In consequence, steam starvation conditions may appear in the lower part of the test rodlet in the same manner as they appear at a distance from the primary defect in a rod in a power reactor (Fig. 1).

3.2 Simulation of primary defect

In order to avoid contamination of the test loop in the DEF and DEFEX tests, the intrusion of water through a primary defect was simulated by applying a water reservoir in an extended plenum on top of the rodlet (Fig. 2). The reservoir was connected to the upper plenum in the test rodlet by a narrow tube. Detection of fission products in the coolant would be a sign of cladding failure. On the other hand, if the cladding remained intact, it would be possible to analyze the released fission gases and the free hydrogen which were retained in the test rodlet. In the first 18 experiments the amount of water in the reservoir was around 0.8 cm^3 , out of which 0.2 cm^3 evaporated as the rodlet was inserted into the test loop. The pressure increase caused the steam to pass through the tube down to the fuel stack. In consequence, at the beginning of an experiment the water vapor was distributed along the fuel stack, and the supply of water was not exhausted during the course of the test (Fig. 3).

This test technique worked well but it had some disadvantages. Firstly, it was necessary to handle the test rodlets vertically. Otherwise there was a risk that the water would flow through the pipe and reach the fuel stack. It would then not be possible to provide an irradiated rodlet with an extra plenum, since this operation is done with the rodlets in a horizontal position in the Hot Cell Laboratory. Secondly, as was mentioned above, this test technique represents a case when the rodlet is already filled with steam as the reactor power is raised.

3.3 The new type of water capsule

In order better to simulate defection of a rod during operation, the technique was modified in the last two tests with irradiated fuel. The new way of simulating the primary defect entails a closed ampoule containing water in the extended plenum (Fig. 2). On one side of the ampoule the wall has been milled down and the wall thickness decreased to 0.15 mm (Fig. 4). The ampoule is filled with an accurately determined amount of water. To cause the ampoule to burst the temperature of the water is increased. The resulting decrease of

the density of the water makes the water fill the ampoule completely at a certain temperature. Further increase of the temperature will result in a rapid pressure increase causing the milled wall of the ampoule to break (Fig. 5). In practice the temperature of the water in the ampoule is controlled by the temperature of the test loop. The rodlet is inserted into the test loop at a temperature which is below the temperature, about 250 °C, at which the ampoule is filled with water. The reactor power is then raised to the operational value. Only when the test rodlet has been irradiated at full power for a predetermined period of time is the ampoule made to burst by increasing the loop temperature to the design value of 275 °C for rupturing the thinned wall (Fig 6). At this moment the pressure outside the ampoule is so low that the water is vaporized when the ampoule breaks. The steam enters the extended plenum, passes through the tube and reaches the fuel stack from above. Upon oxidation of the fuel and the cladding it is reduced to hydrogen which diffuses downwards, hydriding the cladding in the lower part.

The extra plenum equipped with the open water reservoir, or with the ampoule with water, was fabricated in the workshop in the R2 workshop. The extra plenum was welded to the rodlet in the Hot Cell Laboratory using the STUDEFAB process. The irradiated rodlets in the DEMO tests were taken from a stringer rod which had been irradiated in the Ringhals 1 nuclear power plant to a burnup of 25 - 27 MWd/kgU.

4 Test procedure

4.1 Design parameters

Apart from the type of cladding, the design parameter that was varied in the DEF and DEFEX test rodlets was the gap between the cladding and the fuel pellet stack. The fuel in the DEF tests, which was manufactured with standard precision, had a nominal gap of 150 μm , but the DEF-1.2 rodlet had a somewhat larger gap. The DEFEX test rodlets were manufactured with as high precision as possible with regard to the size of the gap. Two values were chosen: 80 μm and 150 μm . A few of the rodlets were manufactured with only the middle section having the lower value, the upper and lower parts having 150 μm gap (Table 1). The nominal gap in the DEMO tests was 200 μm , but the residual gap after irradiation was not measured and remains unknown.

4.2 Experimental parameters

The main experimental parameter was the linear heat rate, LHR, which was varied in various ways. Because of the peaked power profile of the R2 reactor, the maximum LHR value, which is given in the following text, corresponds to an average value which is 0.85 of the maximum. In six of the DEF tests the LHR was 45 kW/m, the last test having a slightly higher value due to a hafnium shield around the bottom part. The seventh DEF test was run at 50 kW/m. In the DEFEX tests the LHR was varied systematically between 26 and 50 kW/m. One of the DEFEX tests and the two DEMO tests entailed stepwise increase of the LHR, starting from 35 or 40 kW/m, when hydriding or failure was believed to have occurred (Table 1).

The irradiation time was the other experimental parameter. The first five DEF tests were allowed to continue for a full operational cycle of the reactor, that is around 17 days. The two last DEF tests were much shorter. Since the rodlets failed in the first DEFEX tests after less than 100 hours, the irradiation time was carefully chosen in the later tests, and the LHR was lowered in order to obtain data on the hydriding of intact fuel. The irradiation time of the DEMO tests was also determined by the time to failure.

5 Results

5.1 Outcome of tests

During irradiation the change in length of the rodlets was measured on-line. The features of the elongation curves thus obtained are considered to reflect the phases of the reduction of steam and subsequent internal hydriding of the cladding. The elongation curves for the DEFEX-1, -2, -3, -4, -5, -8 and -9 as examples are compared in Figure 7. All the elongation curves exhibit the same general shape. Due to the power increase, there was an initial elongation followed by a relaxation period. If the test was allowed to continue, there was a gradual, monotonous increase in length of the rodlet.

The DEFEX-2 rodlet was dissimilar to the rest of the rodlets in that it did not contain any water. It should be noted that the relaxation of this dry rodlet was slower than the relaxation of the other DEFEX rodlets, since the hydrogen and steam mixture gave a better gas conductance than only helium. The long-time increase in length of the wet rodlets can be explained by the hydrogen being consumed by the cladding and replenished by steam. Other phenomena contributing in the same way are irradiation growth and decrease in the thermal conductivity of the fuel due to oxidation. The long-time behavior of the dry rodlet is ascribed to irradiation growth.

Defection of the cladding was accompanied by a spike in the elongation curve, since the ingress of water through the crack decreased the gap conductivity and increased the temperature of the rodlet, before any test loop activity was detected. The curves for the DEMO-1 and -2 tests are given as examples in Figure 8 and 9, respectively. It can be seen that each ensuing step increase of the LHR caused a corresponding release of radioactivity.

In general, as can be seen from Figure 7, the elongation curves of those DEFEX rodlets that failed show a sharper increase than those of the intact ones. In contrast, the DEMO rodlets with medium burnup fuel do not show the same behavior. This could be explained if it is assumed that hydriding starts early in the tests, as was concluded from the DEF-2 test, and further that the cladding of unirradiated fuel will absorb hydrogen easier than cladding of fuel which has attained some burnup. Visual inspection of the hydride aggregates in the defected DEFEX rodlets show that they are larger, causing more deformation than the aggregates in the DEMO rodlets. Several cracks appear in the hydrides in the DEFEX rodlets, but they do not propagate outside the hydrided region in contrast to the cracks in the DEMO rodlets. It seems that the hydriding process was more violent in the unirradiated DEFEX rodlets than in the DEF and DEMO rodlets. This observation may be ascribed to the fact that the DEFEX tests were conducted in such a way that the possibility for forming a protective oxide layer on the inside of the cladding before full LHR had been obtained was minimized.

The crack that appeared at the bottom of the DEMO-1 rodlet was unique in that it grew laterally, going halfway around the circumference. The DEFEX-1, -3, -4, -5 and the DEMO-2 rodlets all exhibited longitudinal cracks.

Figures 10 and 11 show the cracks which developed in the DEMO-1 and -2 rodlets.

Neutron radiography, eddy current scanning and profilometry measurement showed that most of the hydrides and the cracks developed in the lower part of the rodlets, where steam starvation conditions were most likely to occur. Since the pellet - cladding gap was closed along a large part of the rodlets if the local LHR was large enough, hydrides could also develop around the middle of the rodlet.

5.2 Post-irradiation gamma scanning

Gamma scanning of the rodlets was performed after each test in order to determine the distribution of fission products and the average power profile during irradiation. It was found that, with the exception of the DEFEX-3 rodlet, fission products such as ^{131}I , ^{132}Te and ^{140}La were retained in the fuel pellets in the DEFEX rodlets. In contrast, the gamma scans of the DEFEX-3 rodlet clearly showed that the isotope ^{132}Te had migrated to the gaps between the pellets. A similar tendency could be seen for ^{131}I , too. The reason was probably the relatively long irradiation time of 281 hours at a LHR of 50 kW/m. The DEMO rodlets, which had obtained a medium burnup, did not exhibit quite the same distribution. Although most of the iodine, tellurium and lanthanum remained in the pellets, the scans showed that part of the isotopes ^{131}I , ^{132}Te and ^{140}La had assembled in the gaps.

5.3 Post-irradiation SEM analysis

The gamma scans were also used to decide the locations of the samples to be used for SEM, optical spectroscopy and X-ray powder diffraction investigation. Usually two samples were extracted at locations with the same power level above and below the location of maximum LHR. From each of the three DEF rodlets that were subjected to destructive PIE an additional sample for SEM analysis was taken from a position close to power maximum. Samples for SEM analysis were also taken from seven DEFEX rodlets, and from each of the DEFEX-8 and -9 rodlets an additional sample was taken at an elevation above the pellet stack, in the plenum. A total of 25 SEM samples were examined in the backscattering mode, and from the resulting pictures the oxide thickness and the hydrogen contents of the cladding were determined. The hydrogen pick-up fraction was arrived at by relating the hydrogen contents of the cladding to the amount produced from oxidation of the inside and outside of the cladding. The oxide was found to be very porous, so the thickness values were corrected accordingly. The results are given in Table 2.

The measured internal oxide layer in the DEF and DEFEX tests rodlets was never more than 5 μm thick after correction for its porosity. The porosity of the oxide was somewhat less in the rodlets with liner cladding. Further, oxidation seemed to occur preferentially along the grain boundaries of the liner.

As expected, considering the availability of steam in the DEFEX rodlets, the oxide layer was thicker at the upper elevations than at the lower elevations. The fact that the oxide layers were very thin in the DEFEX-8 and -9 rodlets at the locations above the fuel stack, in the plenum, is ascribed to the lower temperature in the plenum and the short irradiation time. The absence of fission product bombardment in the plenum may have had some influence, too.

In the DEF rodlets the oxide layer was usually thickest at the middle position, where the LHR and the temperature were highest. The difference in oxide layer thickness with elevation was not as pronounced in the DEF-1.1 and -2.2 rodlets as it was in the DEF-2.4 and DEFEX rodlets. This observation can be explained by the fact that the two tests DEF-1.1 and -2.2 lasted for a much longer time than the DEF-2.4 and DEFEX tests, thus permitting enough steam to reach the bottom part and oxidize the cladding.

In the DEFEX-3 rodlet the relatively large oxide layer thickness at the lower elevation can be explained by the fact that the irradiation continued for some time after defection, thus allowing external water to enter the rodlet through the crack.

Comparing the results of the SEM measurements of the rodlets from DEFEX-1 and DEFEX-4, which were run for approximately the same time, it is seen that, although the oxide layers at the upper elevation were equal, the oxide layers at the lower elevation were four times as thick in the DEFEX-4 rodlet. In fact, since the DEFEX-1 rodlet was actually irradiated for one hour after defection, the difference should perhaps be even higher. This is an indication that the design with rifled cladding to some extent fulfilled its intended purpose to facilitate axial gas communication.

In the tests DEFEX-5X and DEFEX-6 the behavior of a rodlet with standard cladding was compared to a rodlet with liner cladding under identical conditions. The irradiation time being short, the oxide did not grow much. Nevertheless, the rodlet with liner cladding had a thinner oxide layer than the rodlet with standard cladding (at the higher elevation).

The tests DEFEX-8 and DEFEX-9 were also intended to demonstrate the difference in behavior between standard cladding and cladding with liner under equal conditions. The oxide layer at the lower elevation was somewhat thicker in the rodlet with liner cladding than in the rodlet with standard cladding. On the other hand, the oxide layer at the upper elevation was thicker in the standard cladding rodlet. Note, however, that the hydrogen pick-up was much larger in the standard cladding rodlet.

Caution should be exercised when comparing the DEF-1.1 and -2.2 rodlets, since the former was of an older design than the DEF-2 (and DEFEX) rodlets. The irradiation conditions being approximately equal, the difference in oxidation behavior seems to be slight.

In some cases the hydrogen pick-up was found to be above 100 %. The reason for this is that in these cases some of the free hydrogen in the rodlet had also been absorbed into the cladding.

5.4 Post-irradiation ceramography

Ceramography of the DEF-1.1 and -1.2 and the DEFEX-1, -3, -4, -8 and -9 rodlets was done optically for porosity and grain size measurement. It was found that the fuel grain size increased more in the top samples than in the bottom samples from the DEFEX-3 and -4 rodlets, which were irradiated at the same LHR. The largest increase was seen in the DEFEX-3 rodlet, which was irradiated almost three times as long. From the DEFEX-1 rodlet only a top ceramography sample was taken, which exhibited grain growth amounting to a value between what was seen in the DEFEX-3 and -4 rodlets. The grain growth in the top samples is attributed to oxidation of the fuel, which increases all diffusion coefficients. On the other hand, no grain growth was seen in the samples from DEFEX-8 and -9, probably because of the low LHR. The DEF-1.2 rodlet showed grain growth in the center, which was somewhat larger than the grain growth in the DEF-1.1 rodlet. This is an indication of a higher O/U ratio in the DEF-1.2 rodlet. However, it should be pointed out that the two rodlets were not of the same manufacture.

Porosity distribution in the DEFEX-1 top sample and in the samples from the DEFEX-4 rodlet show densification in the center. In contrast, in the DEFEX-3 samples the increase in porosity in the center was offset by the formation of intergranular gas bubbles.

5.5 Post-irradiation stoichiometry measurement

X-ray powder diffraction was used to determine the value of x in the oxidized uranium dioxide UO_{2+x} . Samples, 10 in all, were taken from an upper level of the DEFEX-2 and -4 rodlets and from two levels with the same LHR of the DEFEX-1, -3, -8 and -9 rodlets. Fragments of pellet were extracted, and from these several X-ray powder specimens were prepared. Peripheral specimens could be discerned; the location of other specimens in the interior could not be determined. The specimens were then exposed, two at a time, in a pair of Guinier-type focusing cameras. From the diffraction patterns the lattice parameter of the cubic structure was obtained. The high accuracy and reproducibility of the measurements is indicated by the fact that the difference in lattice parameter values obtained from the two cameras was usually within one standard deviation. The lattice parameter a_0 is related to the value of x through the so-called Vegard's equation:

$$\delta x = \delta a_0 / K_V \text{ with } K_V = -0.148 \text{ \AA per atom O.}$$

δa_0 is the difference in lattice parameter between the value = 5.47150 Å for stoichiometric $\text{UO}_{2.00}$ and that measured for the specimen. δx is the shift in oxygen content relative to $\text{UO}_{2.00}$.

Analysis of an unirradiated sample gave a value of x in UO_{2+x} which varied from 0.0031 in the center to 0.0039 at the periphery. 6 samples from the dry rodlet in DEFEX-2 were analyzed in order to obtain the influence on the lattice parameter and hence on the value of x from irradiation and fission products. It was found that the lattice had expanded somewhat at the periphery despite the short irradiation time of approximately 13.5 days at 50 kW/m. In the center it seemed that the irradiation damage had been partly repaired due to temperature annealing. Assuming that the dilation of the lattice is directly proportional to the burnup, and consequently to irradiation time and LHR, the values of x for the wet rodlets were corrected accordingly when applying Vegard's equation. The results are presented in Table 3.

The hyperstoichiometry increased with increasing irradiation time, the upper sample generally exhibiting larger values because of the availability of steam. However, the values from the DEFEX-3 rodlet coincided in mean and range. The reason is probably that during the relatively long duration of the test abundant steam could penetrate to the bottom part and enter through the crack in the bottom.

5.6 Post-irradiation analysis of internal gas

Upon puncturing the rodlet in the plenum, the pressure of the internal gas collected in a standard volume was determined. The composition of the gas was measured by mass spectroscopy.

The results of the internal gas analysis are given in Table 4. The measured amounts of hydrogen in the DEFEX rodlets are compared to the values calculated with INTERPIN.DF, which is a LWR fuel rod performance code, designed to handle the case of defective cladding. It is an expanded version of the INTERPIN code for general fuel performance analysis [8].

The PIE analysis of the internal gas gave the amounts of hydrogen and helium which were the main components. Release factors for fission gases such as krypton and xenon were also determined. Small amounts of methane and nitrogen were detected.

The measured amounts of He were consistent with the specifications considering that the measured free volume was around 11 cm^3 for all the rodlets, except for the DEF-2.5 rodlet, which had 12.8 cm^3 . There are variations in the helium values, however, indicating either that the filling procedure may not have been perfect, or that some gas may have been lost due to leakage or when the rodlets were punctured.

The amount of free hydrogen generally increased with the duration of the irradiation. It was evidently influenced by the amount that went into the cladding. The fact that UO_2 samples have been found whose values are close to that of the unirradiated uranium dioxide and the fact that the internal oxide thickness was considerably less in the bottom than at the upper elevation in most of the DEFEX tests show that the hydrogen/steam ratio locally had

become high enough in some of the tests to suppress further oxidation of the UO_2 and the internal cladding.

The presence of CH_4 is explained by the appearance of traces of carbon in the fuel according to specifications. The presence of N_2 indicates that some air leaked into the rodlet during He and water filling. However, the influence on the internal oxidation as the temperature increased is judged to be slight.

6 Conclusions

Comparing the shape of the elongation curves from the DEF and DEFEX tests it is concluded that hydriding started early, generally a few hours after full LHR was reached, and continued for between two and three days. This is substantiated by the outcome of the DEMO-2 test. The steam starvation condition was no longer fulfilled and the hydriding process was interrupted when more vapor penetrated downwards in the fuel rodlet. The large size of the hydride aggregates in some of the DEFEX rodlets is an indication that the hydriding process is likely to continue for a period of time, since the amount of free hydrogen in the rodlet volume is less than what has been absorbed in the cladding.

Several of the tests resulted in cracks in the cladding, all of them starting in hydride aggregates. No indication was found of the cracks growing into the region outside the aggregates in the DEFEX rodlets despite the maximum LHR being as high as 50 kW/m. In contrast, the cracks in the DEMO rodlets continued into the unhydrided region at the same LHR. It is suggested that the difference could be attributed to the cladding being more brittle due to irradiation in the DEMO rodlets.

There was no significant difference in the oxidation behavior of the liner cladding and the standard cladding.

References

- 1 "Review on fuel failures in water reactors", *IAEA technical report*, to be published.
- 2 H. Mogard, M. Grounes, H. Tomani, "Irradiation investigation of the initial phase of degradation of BWR type fuel rodlets containing simulated single fretting clad defects", *Enlarged Halden Programme Group Meeting on Fuel and Materials Performance*, Bolkesjö, Norway, June 9-14, 1991.
- 3 H. Mogard, M. Grounes, G. Lysell, H. Tomani, "Experimental studies of post-failure degradation of BWR fuel rodlets", *Proc. International Topical Meeting on Light Water Reactor Fuel Performance*, West Palm Beach, Fl, USA, April 17-21, 1994, pp 423 - 434.
- 4 C. Gräslund, G. Lysell, K. Ogata, T. Takeda, "Studies of the secondary hydriding process in fresh test fuel with simulated primary defects", *ANS 1997 International Topical Meeting on Light Water Reactor Fuel Performance*, Portland, Oregon, USA, March 2-6, 1997, pp 342 - 349.
- 5 C. Gräslund, G. Lysell, "The behaviour of 8x8 BWR test fuel with simulated primary defects", accepted for *TOPFUEL '97*, 9-11 June 1997, Manchester, UK.
- 6 R. W. Stratton, A. Pagani, H. U. Zwicky, "Defect fuel experience in Switzerland since 1985 (without Mühleberg)", *AEA IWG on (Water Reactor) Fuel Performance and Technology*, 9-11 May 1994.
- 7 R. L. Yang, O. Ozer and H. H. Klepfer, "Fuel performance evaluation for the EPROM program planning", *ANS/ENS International Topical Meeting on LWR Fuel Performance*, Avignon, France April 21-24 1991, Vol 1, pp 228-271.
- 8 N. Kjaer-Pedersen, "A Novel Fuel Rod Performance Simulation Methodology for Predictive, Interpretative and Educational Purposes", *Res Mechanica* 25 (1988) 321-338.

Test No	LHR max. (kW/m)	Irradiation time/ (time to failure)	Gap (μm)	Remarks	Type of Zircaloy-2 cladding
DEF-1.1	45	16½ days	150	hydride, intact, scram	older standard
DEF-1.2	45	17 days	200	intact, scram	rifled
DEF-2.1	45	17 days	150	intact	standard
DEF-2.2	45	15 days	150	intact	liner
DEF-2.3	45	17½ days	150	intact	rifled
DEF-2.4	50	1 day	150	intact, hydride	standard
DEF-2.5	46	4½ days	150	Hf shield at bottom	rifled
DEFEX-1	50	90/(88) hrs	150	hydride, crack	standard
DEFEX-2	50	272 hrs	150	dry, intact	standard
DEFEX-3	50	281/(216) hrs	150	hydride, crack	liner
DEFEX-4	50	(102) hrs	150	hydride, crack	rifled
DEFEX-5	40	(76) hrs	150	hydride, crack	standard
DEFEX-5X	40	12 hrs	80/150	hydride	standard
DEFEX-6	40	12 hrs	80/150	intact	liner
DEFEX-7	26	76 hrs	80	intact	standard
DEFEX-8	30	167 hrs	150	intact	standard
DEFEX-9	30	168 hrs	150	intact	liner
DEFEX-10	40/62	48/1 hrs	80	intact, ramped	liner
DEMO-1	35/40/45	(6 days + 9 hrs)	200	LHR step increase, 25 MWd/kgU, hydride, crack	standard
DEMO-2	40/45/50	(49 + 3 hrs)	200	LHR step increase, 27 MWd/kgU, hydride, cracks	standard

Table 1

Overview of DEF and DEFEX tests of fresh fuel and DEMO tests of fuel with medium burnup. Note that some of the DEFEX rodlets had a gap of 80 μm in the middle and 150 μm in the ends.

Rodlet no.	Position (mm from bottom)	Inside oxide (μm)	Hydrogen contents (ppm)	Hydrogen pick-up (%)
DEF-1.1	66	4.5	94	64
	272	5.3	98	56
	427	3.8	81	65
DEF-2.2	66	5.1	71	37
	272	5.2	77	38
	427	4.5	30	16
DEF-2.4	66	0	35	-
	272	2.2	55	76
	427	1.8	69	117
DEFEX-1	68	0.7	186	543
	374	4.3	204	137
DEFEX-3	65	4.4	126	77
	423	4.7	74	36
DEFEX-4	55	2.8	68	61
	403	4.3	76	47
DEFEX-5X	78	0	28	-
	434	1.0	100	305
DEFEX-6	78	0	36	-
	434	0.7	30	131
DEFEX-8	78	1.1	81	225
	434	3.4	211	189
	483	0	14	-
DEFEX-9	78	1.8	53	90
	434	2.6	23	27
	483	0.6	5	25

Table 2

Oxide thickness, corrected for porosity, and hydrogen concentration and pick-up in the DEF and DEFEX rodlets.

DEFEX Test No.	Irradiation time (hrs)	Location (mm fr bottom)	$\times 10^{-4}$ in UO_{2+x} average (range)			
			Internal samples		Peripheral samples	
1	90	68	49	(11 - 94)	31	(7 - 54)
		374	89	(45 - 112)	129	(104 - 153)
3	281	65	100	(95 - 107)	185	(168 - 204)
		423	106	(84 - 127)	190	(173 - 207)
4	102	55	74	(62 - 88)	101	(79 - 122)
8	167	77	20	(9 - 29)	61	(39 - 82)
		433	97	(84 - 104)	88	(49 - 111)
9	168	77	15	(12 - 18)	37	(5 - 60)
		433	45	(43 - 47)	85	(76 - 94)

Table 3
Stoichiometry Shifts for Peripheral and Internal Samples in the DEFEX Rodlets.

Rodlet no.	H_2 (NTP cm^3)		He (NTP cm^3)	N_2 (NTP cm^3)	CH_4 (NTP cm^3)	Kr %	Xe %
	measured	calculated					
DEF-1.1	114.9	-	6.0	0.22	-	9.0	8.4
DEF-2.1	196.9	-	9.5	0.08	-	3.8	3.6
DEF-2.2	230.7	-	7.8	0.27	-	0.8	0.9
DEF-2.3	195.6	-	7.9	0.45	-	1.1	1.2
DEF-2.4	46.0	-	7.8	0.63	-	0.8	0.8
DEF-2.5	152.5	-	5.8	2.19	-	0.5	0.4
DEFEX-3	73.5	292	45.9	0	-	12	9
DEFEX-5X	21.1	36	56.4	0.30	-	-	-
DEFEX-6	35.1	43	50.2	3.11	-	-	-
DEFEX-7	62.7	-	54.9	2.44	0.22	-	-
DEFEX-8	138.9	125	43.9	2.67	0.75	0.5	0.4
DEFEX-9	132.0	155	52.6	1.56	1.52	0.6	0.4
DEFEX-10	34.8	-	50.4	2.89	0.88	1	1

Table 4
Measured amounts of remaining hydrogen, He, CH_4 and N_2 , and release factors of Kr and Xe in the intact DEF and DEFEX rodlets. Note that the measured values for the leaking DEFEX-3 rodlet were arrived at by extrapolating with the remaining He pressure as reference. The measured amounts of hydrogen in the DEFEX rodlets are compared to values calculated with INTERPIN.DF.

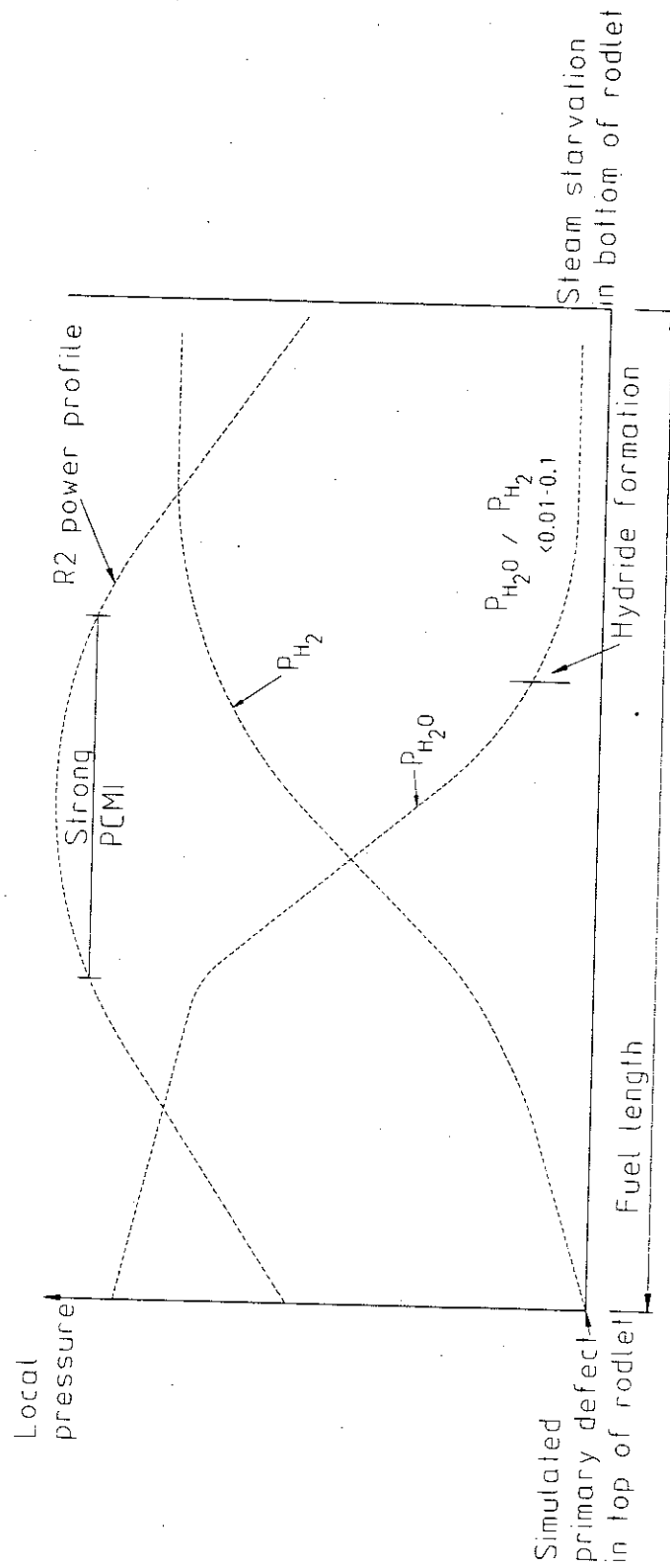


Figure 1
 Conceptual diagram demonstrating how the axial power distribution influences the hydriding process.

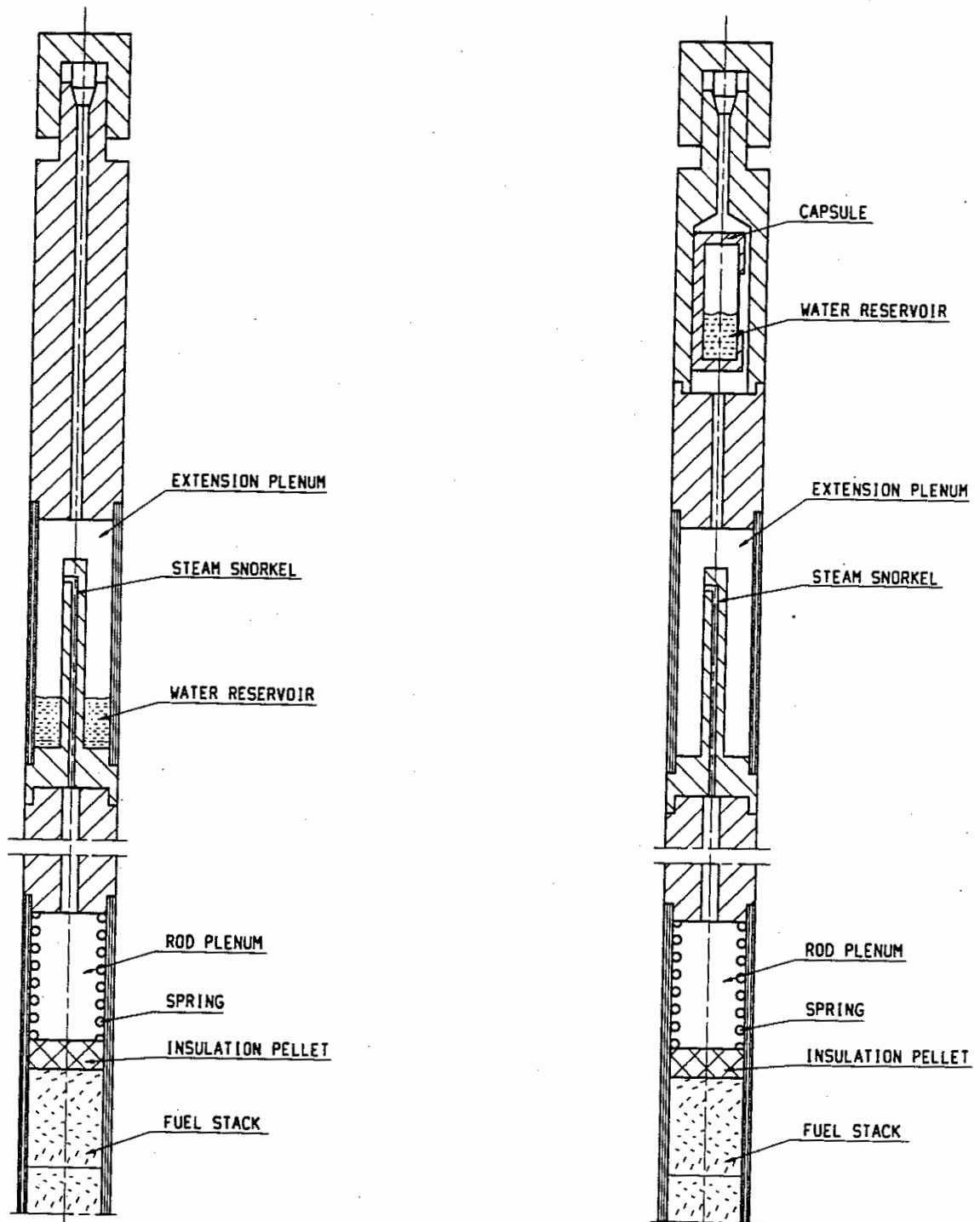


Figure 2

Array simulating primary defects in fuel. Left: design used in the DEF and DEFEX tests; right: improved (modified)

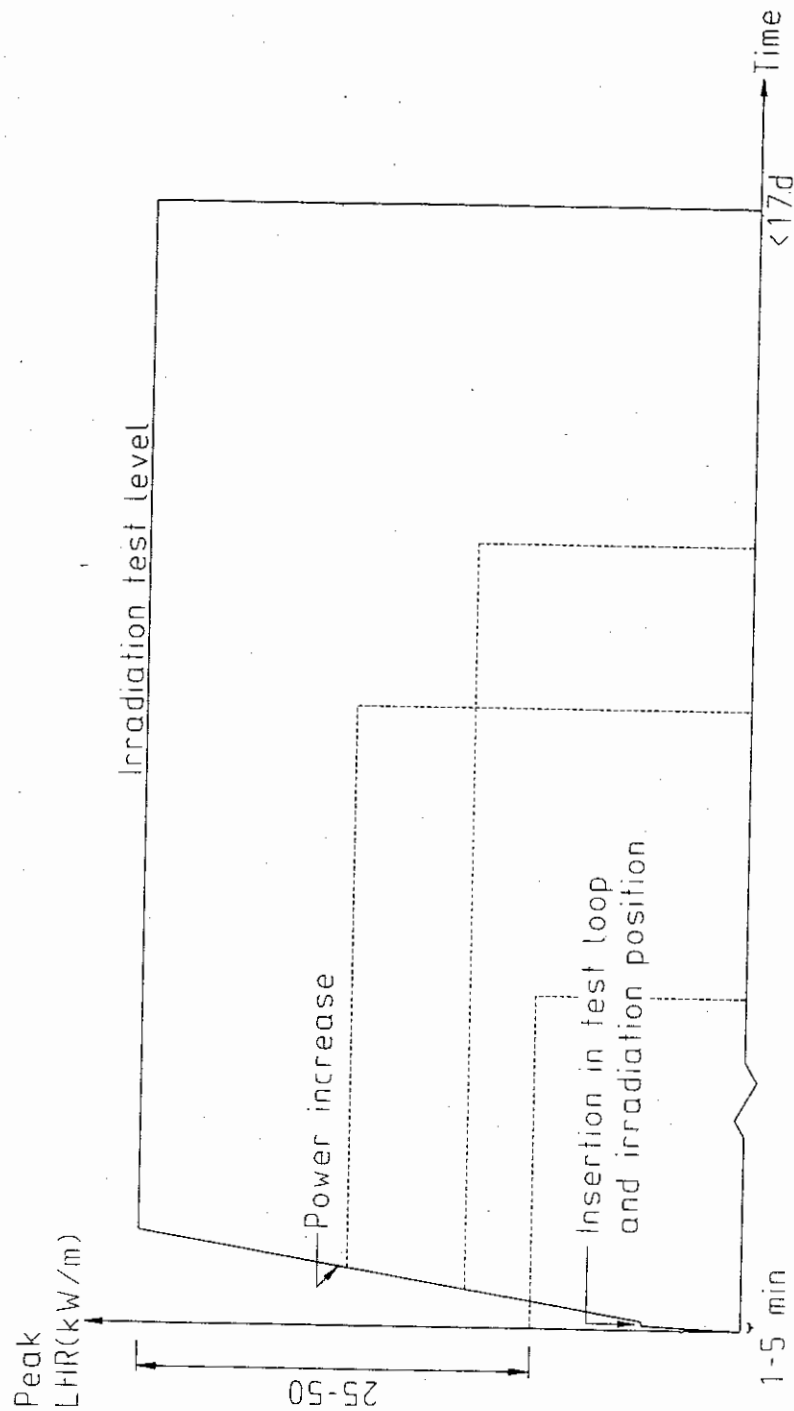


Figure 3

Schematic test scheme of the DEFEX Project.

As the rodlet was lowered into the test loop, the temperature increase caused part of the water in the reservoir in the extended plenum to turn into steam, which filled the interior of the rodlet. When the rodlet was further lowered into the irradiation position it was held at a LHR of about 19 kW/m for as short a time as possible, between 1 and 5 minutes. The power of the rodlet was then increased at a rate of 3 kW/m-min to a predetermined level, which for the DEFEX tests varied between 25 and 50 kW/m. The tests lasted for less than a reactor period.

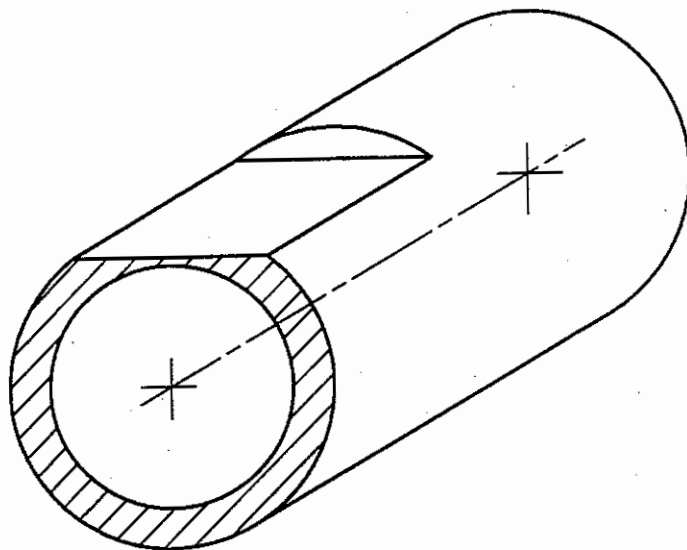
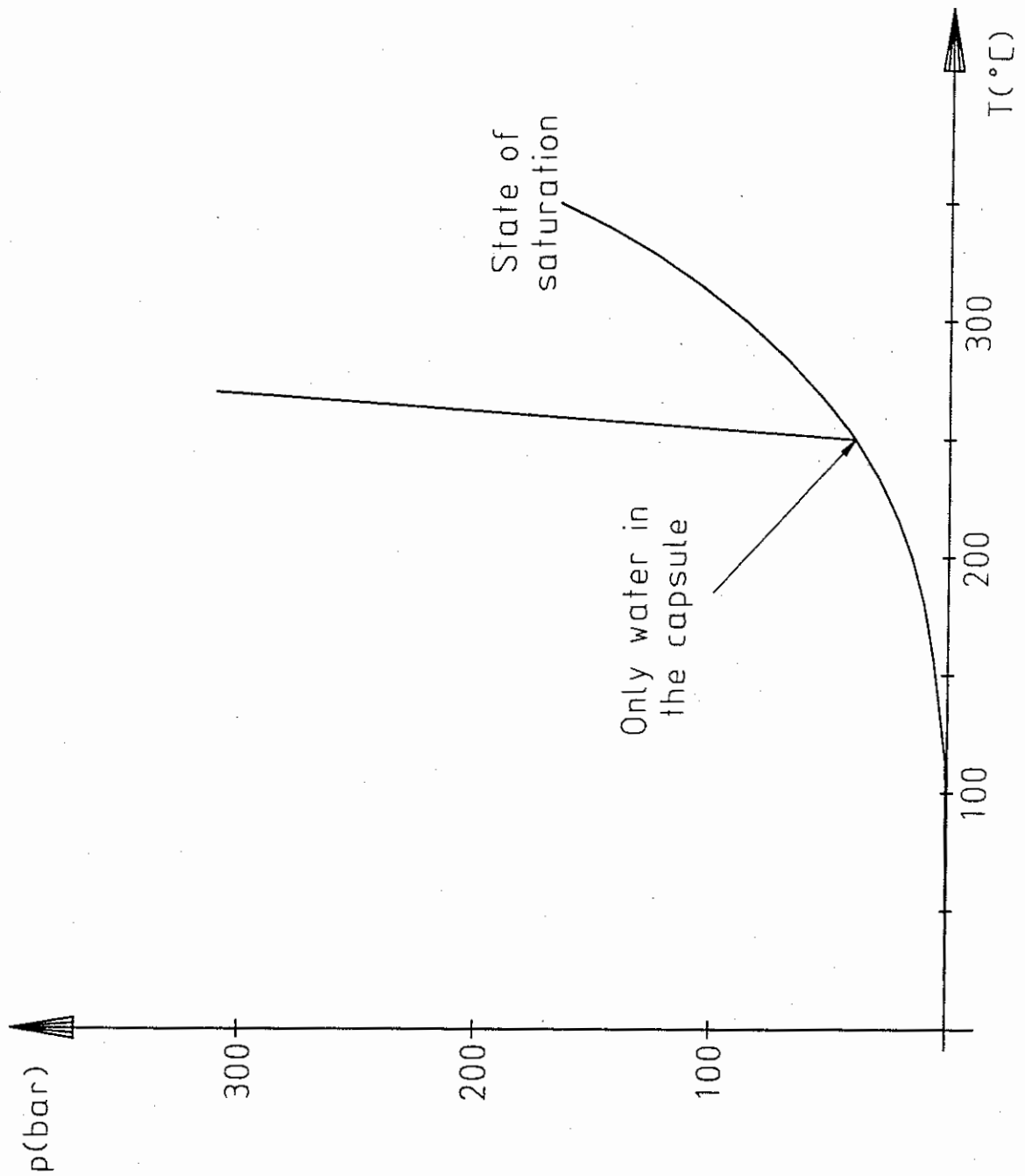


Figure 4

The water ampoule with its milled thin side, which was used in the modified technique for simulating a primary defect in the DEMO tests.

**Figure 5**

Pressure vs. temperature when the thinned wall of the ampoule is made to burst.

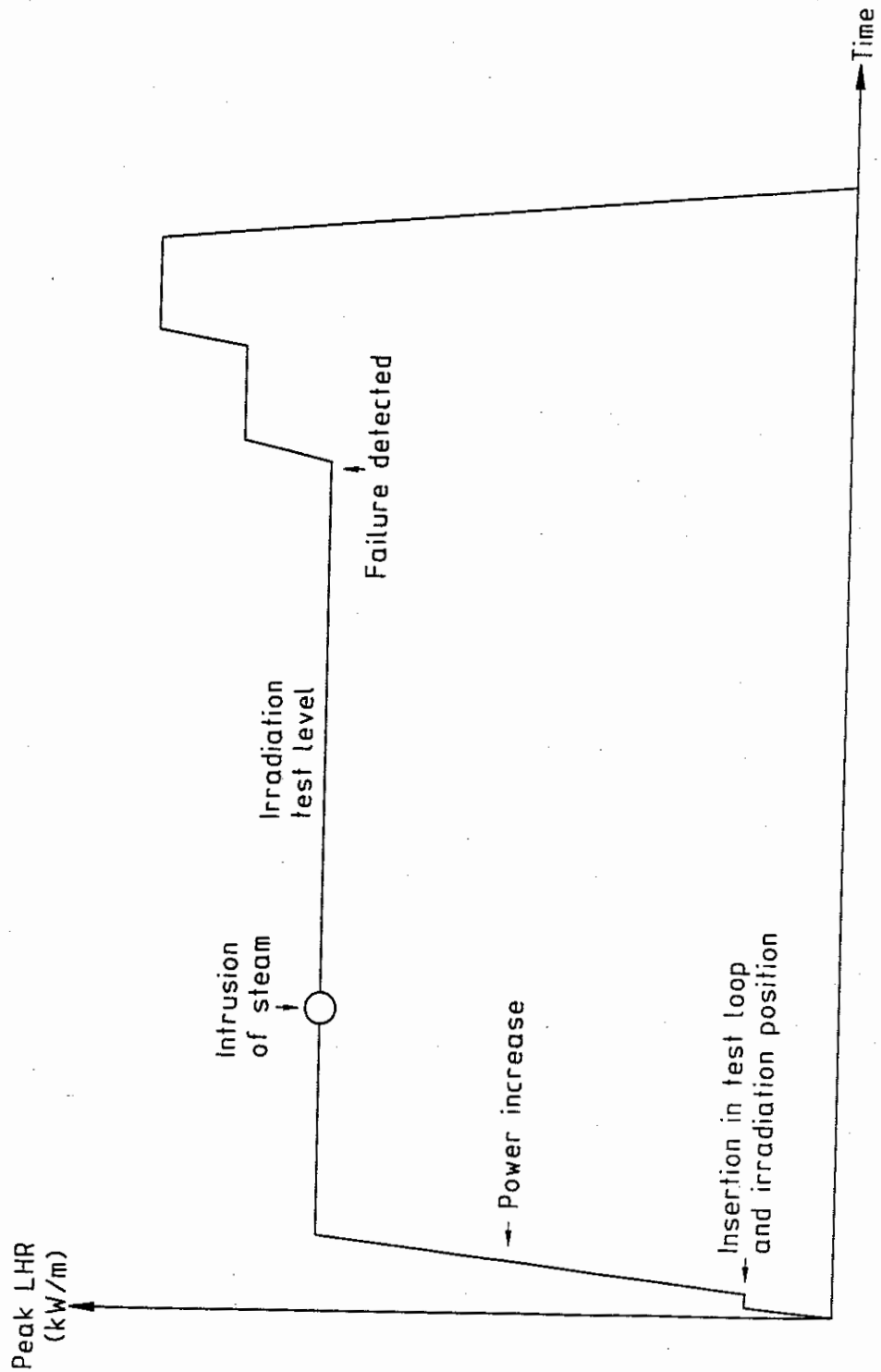


Figure 6

Schematic test scheme for the DEMO tests. The LHR is increased step-wise when the activity level in the test loop increases, signaling failure of the cladding

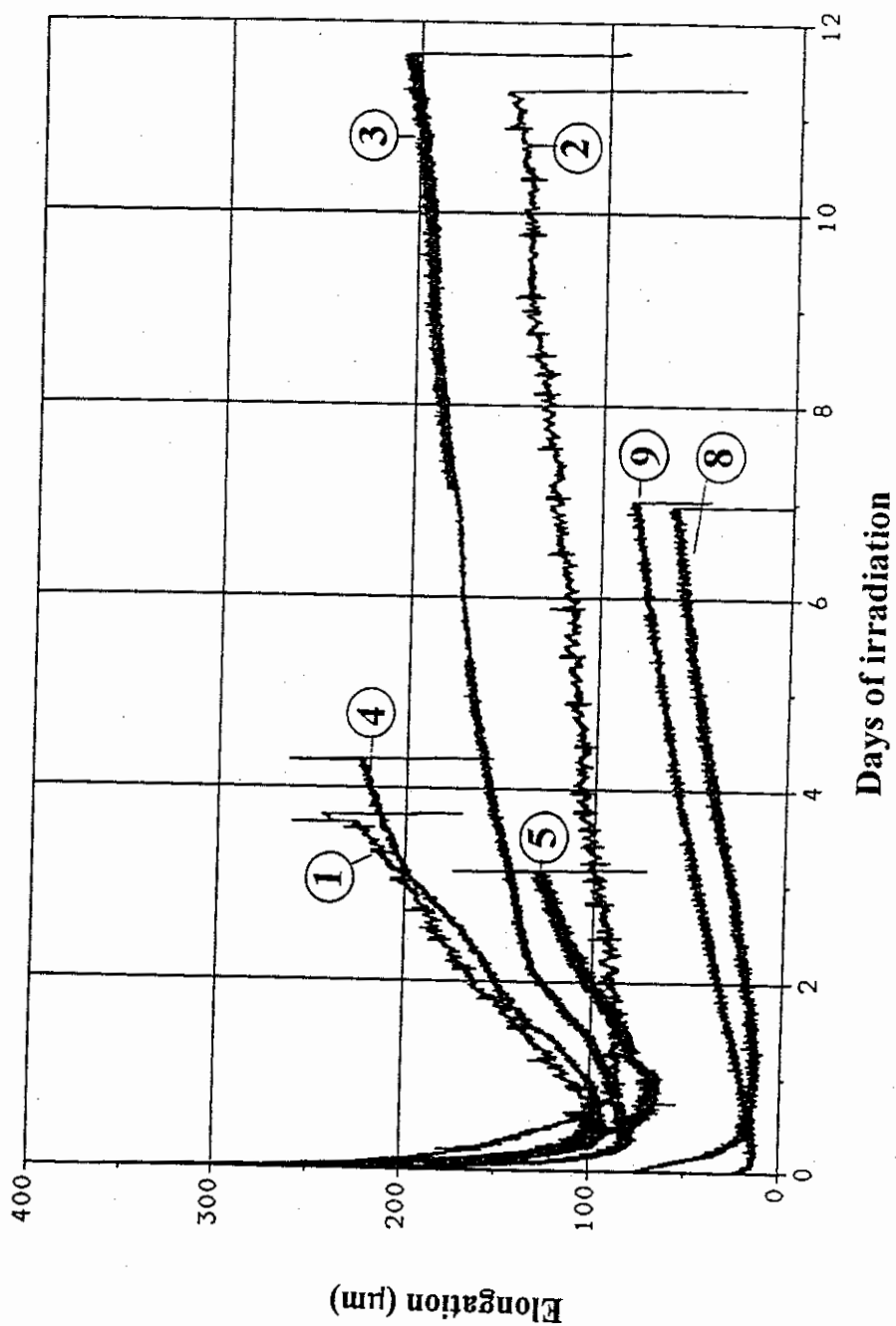


Figure 7
Comparison of the elongation curves from the DEFEX-1, -2, -3, -4, -5, -8 and -9 tests.

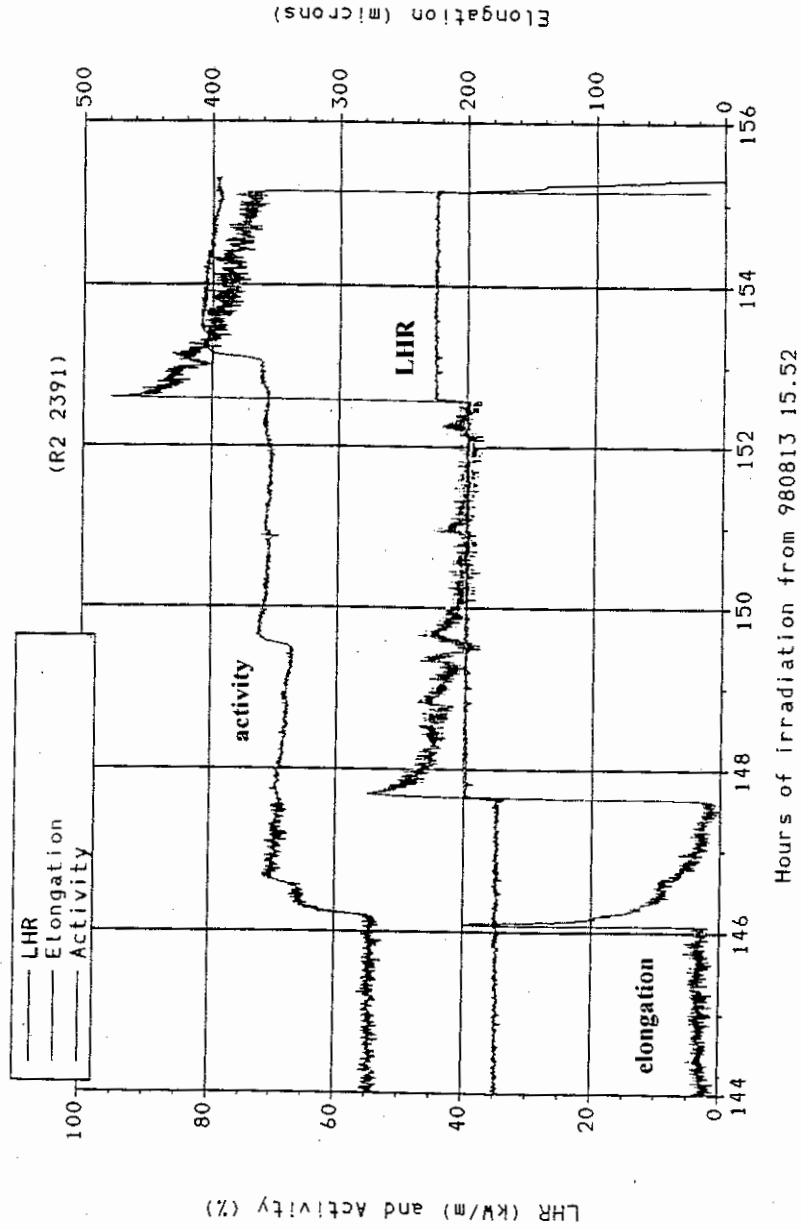


Figure 8
Irradiation history for the DEMO-1 test during the last 12 hours.

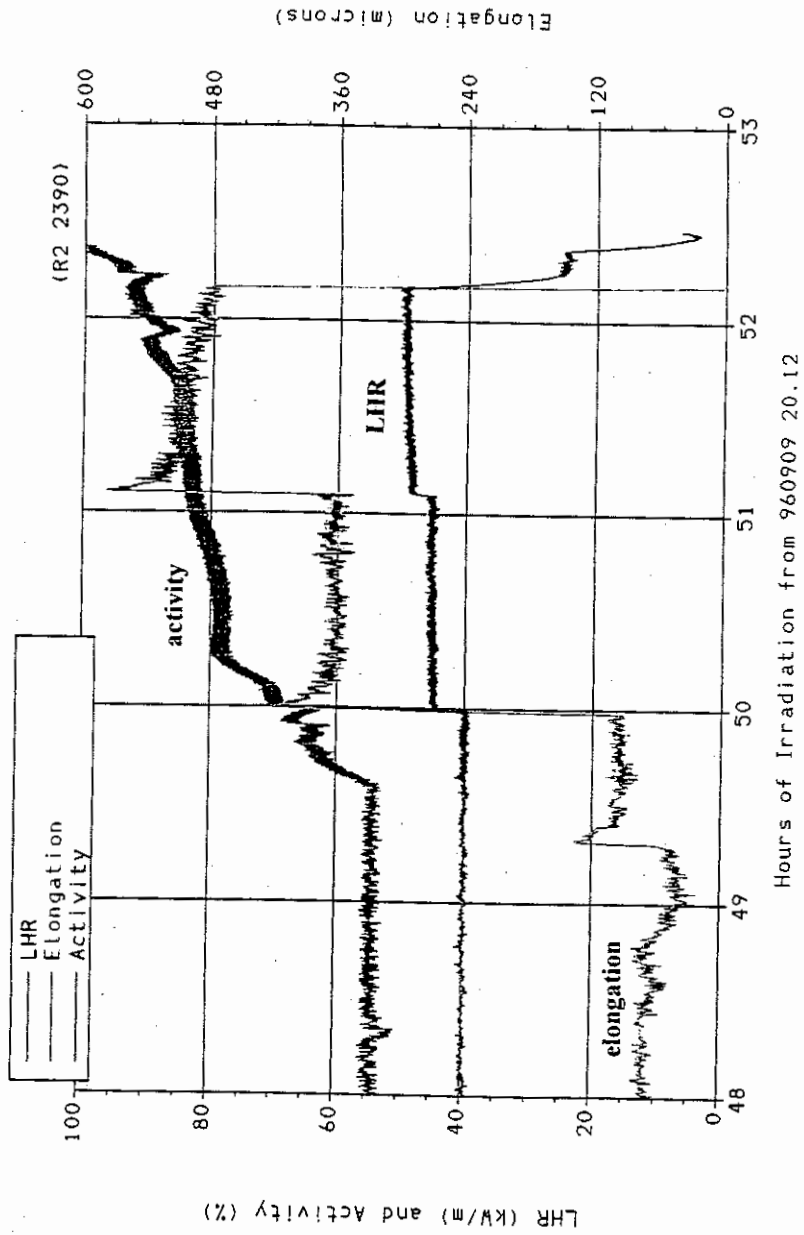


Figure 9
Irradiation history for the DEMO-2 test during the last 4 hours.

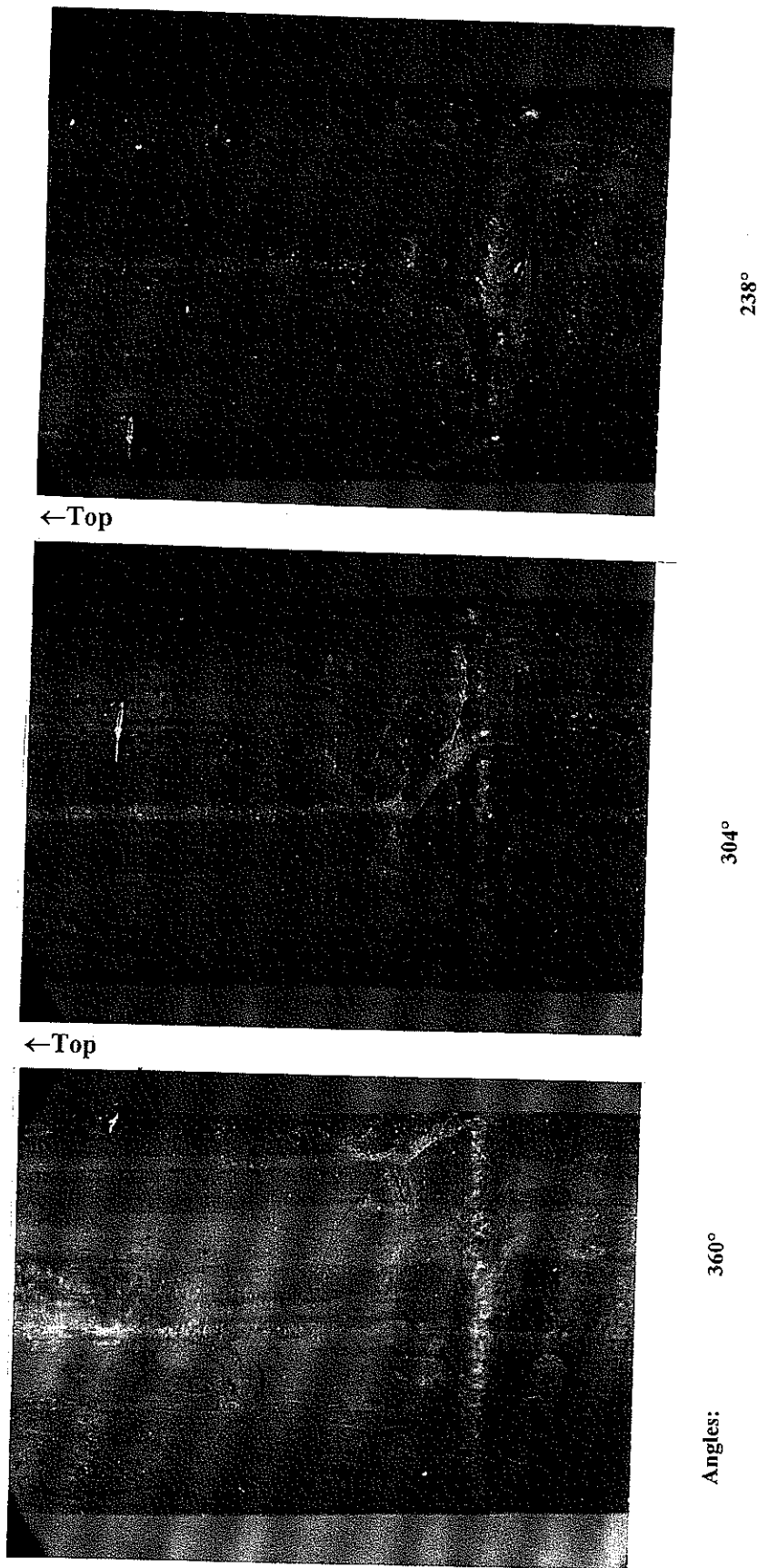


Figure 10
Photos in 5x magnification of bottom end of rodlet 2391 from DEMO-1 at consecutive angles showing large crack in hydride.

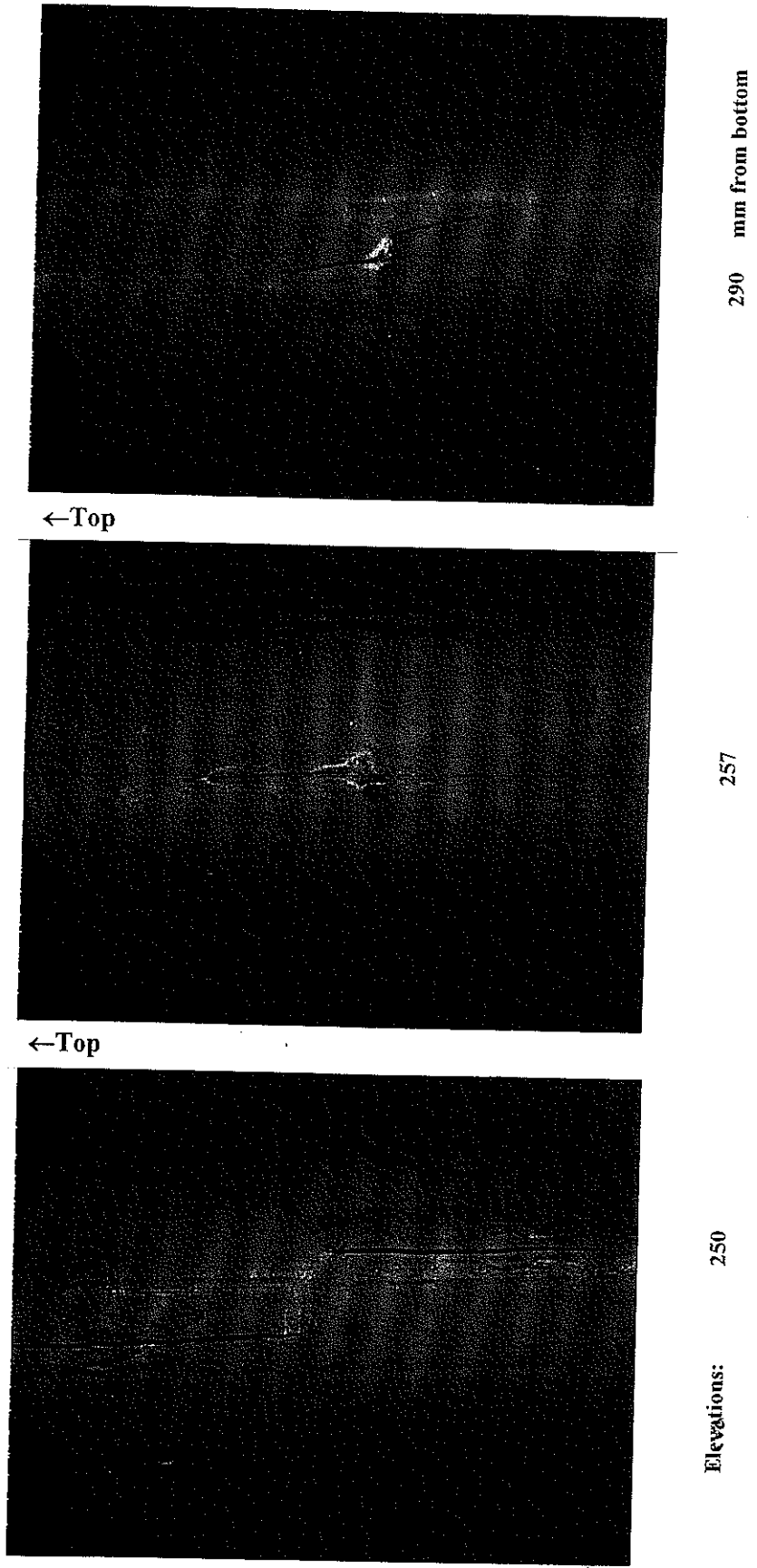


Figure 11
Photos in 4x magnification of rodlet 2390 from DEMO-2 at various elevations showing cracks in hydrides.